ISSN 1674-1056
http://cpb.iphy.ac.cn
http://iopscience.iop.org/cpb
中国物理 B
Chinese Physics
中国物理 Chinese Physics B

Similarity principle of microwave argon plasma at low pressure

Xiao-Yu Han(韩晓宇), Jun-Hong Wang(王均宏), Mei-E Chen(陈美娥), Zhan Zhang(张展), Zheng Li(李铮), Yu-Jian Li(李雨键)

Citation: Chin. Phys. B . 2018, 27(8): 085206. **doi:** 10.1088/1674-1056/27/8/085206

Journal homepage: http://cpb.iphy.ac.cn; http://iopscience.iop.org/cpb

What follows is a list of articles you may be interested in

Preparation of Se-based solar cell using spin-coating method in ambient condition

Menghua Zhu(朱孟花), Yaxin Deng(邓雅心), Weiwei Liu(刘伟伟), Xin Li(李欣)

Chin. Phys. B . 2018, 27(1): 015202. **doi:** 10.1088/1674-1056/27/1/015202

Initial growth and microstructure feature of Ag films prepared by very-high-frequency magnetron sputtering

Yue Zhang(张悦), Chao Ye(叶超), Xiang-Ying Wang(王响英), Pei-Fang Yang(杨培芳), Jia-Min Guo(郭佳敏), Su Zhang(张苏)

Chin. Phys. B . 2017, 26(9): 095206. **doi:** 10.1088/1674-1056/26/9/095206

Effect of driving frequency on the structure of silicon grown on Ag (111) films by very-high-frequency magnetron sputtering

Jia-Min Guo(郭佳敏), Chao Ye(叶超), Xiang-Ying Wang(王响英), Pei-FangYang(杨培芳), Su Zhang(张苏)

Chin. Phys. B . 2017, 26(6): 065207. **doi:** 10.1088/1674-1056/26/6/065207

Preparation and structural properties of thin carbon films by very-high-frequency magnetron sputtering

Ming-Wei Gao(高明伟), Chao Ye(叶超), Xiang-Ying Wang(王响英), Yi-Song He(何一松), Jia-Min Guo(郭佳敏), Pei-Fang Yang(杨培芳)

Chin. Phys. B . 2016, 25(7): 075202. **doi:** 10.1088/1674-1056/25/7/075202

Implicit electrostatic particle-in-cell/Monte Carlo simulation for the magnetized plasma: Algorithms and application in gas-inductive breakdown

Wang Hong-Yu, Sun Peng, Jiang Wei, Zhou Jie, Xie Bai-Song

Chin. Phys. B . 2015, 24(6): 065207. **doi:** 10.1088/1674-1056/24/6/065207

Similarity principle of microwave argon plasma at low pressure*

Xiao-Yu Han(韩晓宇), Jun-Hong Wang(王均宏)†, Mei-E Chen(陈美娥), Zhan Zhang(张展), Zheng Li(李铮), and Yu-Jian Li(李雨键)

Institute of Lightwave Technology, Beijing Jiaotong University, Beijing 100044, *China*

(Received 27 February 2018; revised manuscript received 1 April 2018; published online 10 July 2018)

In order to validate the similarity principle of microwave breakdown, a two-dimensional (2D) fluid model of low-pressure microwave argon plasma is established and solved by the finite-element method. Proportional conditions are used in this model to build three different breakdown processes that meet the premise of a similarity principle, and these breakdown processes are called "similar cases" in this paper. Similar cases have proportionately sized breakdown regions, where the ratio of frequency of incident microwave f to gas pressure p (f/p), and the reduced field E/p in them are kept the same. All the important physical parameters such as electron density, electron temperature, and reduced electric field can be obtained from the simulation of this model. The results show that the parameters between similar cases are in constant ratio without changing with time, which means that the similarity principle is also valid in microwave breakdown.

Keywords: similarity principle, microwave plasma, low pressure, 2D fluid model

PACS: 52.80.Pi, 52.65.–y, 51.50.+v, 52.50.Sw **DOI:** 10.1088/1674-1056/27/8/085206

1. Introduction

Microwave plasmas are widely used in industry for depositing, heating, and coating. Compared with the plasmas generated by classical direct current (DC) or low frequency technologies, the plasmas generated by microwave technology have larger electron density and higher power utilization efficiency.[1,2] However, in the traditional theoretical study of microwave plasma, the time for simulating the breakdown models by fluid-based methods is quite long and the requirement for computation resource is very high, especially for the extreme cases with very high pressure or with large breakdown area. In order to improve the computation efficiency, the methods based on the similarity principle for DC or low frequency plasmas have been put forward.[3,4] With the similarity principle, extreme case problems can be effectively solved by approximating them to general and computable models. However, for microwave breakdown, the premises and effectiveness of the similarity principle are not clear yet.

The similarity principle is a statement of conditions under which similar discharges take place in the determined area. In the past few decades, theories of the similarity principle have been studied by many researchers. Paschen first revealed that the breakdown voltage depends on a constant product pd, where p is the gas pressure and d is the length of the breakdown gap or the distance between anode and cathode.[5] By this theory, a problem with very high pressure can be equivalent to another problem with lower pressure but larger length of breakdown gap. This original general similarity theory was extended by Holm to another problem, in which the potentials were determined by space charges as well as by charges on the electrodes.[6] For high-frequency breakdown, the definition of a similarity law was first given by Margenau in 1948,[7] and then Jones and Morgan studied the high-frequency (3.5 MHz∼70 MHz) breakdown between wires and coaxial cylinders in air and in hydrogen respectively at low pressure (lower than 2.66 kPa). The results proved that Margenau's theory of the similarity principle in high-frequency breakdown is correct, and the parameters of breakdowns with different air pressures and breakdown sizes are kept in certain ratios.[8] Recently, Fu *et al.* carried out numerical simulations to investigate the validity of the similarity principle of argon glow discharges at low pressure, showing that the proportional relation can be given by the similarity law between two discharge gaps, and also extends the traditional Paschen law for the gas breakdowns to non-uniform electric field conditions.[9]

However, very few studies or verifications of a similarity principle for high-frequency problems can be found after the work of Jones and Morgan. Furthermore, it is hard to find the studies of the similarity principle for breakdown problems in microwave-frequency band (300 MHz–300 GHz), although many difficult breakdown problems occur in current high power microwave applications. An equivalent method based on the similarity principle in the microwave band could offer a way to simplify the study of breakdown in a large area into a similar case with a computable proportional small size. From the results of the small sized case, the breakdown parameters of large size problem can be extrapolated.

In this paper, microwave (with frequency higher than 2 GHz) breakdowns in similar processes are studied numer-

*Project supported by the National Natural Science Foundation of China (Grant No. 61331002), the National Key Basic Research Program of China (Grant No. 2013CB328903), and the Fundamental Research Funds for the Central Universities, China (Grant No. W15JB00510).

†Corresponding author. E-mail: wangjunh@bjtu.edu.cn

© 2018 Chinese Physical Society and IOP Publishing Ltd

ically using a two-dimensional (2D) fluid model for verifying the validation of the similarity principle in the microwave band. Parallel plate waveguides are used to build the breakdown region with argon in it as the working gas. By this study, the correctness of the similarity principle in microwave breakdown can be verified comprehensively, and the proportional relations between the important physical parameters, including the electron densities, electron temperature, and the distribution of electric field, of microwave breakdowns in similar cases can be found.

2. Theories of similarity principle in microwave breakdown

2.1. Brief review of similarity principle in DC-discharge

Relations between parameters of two similar systems for DC-discharge, derived under the similarity principle, are listed in Table 1, where k is the scale-down ratio. The dominant processes in the breakdown are the collisions between electrons and argon atoms, the diffusion and drift of the electrons and ions. The microcosmic physical parameters used to describe this process are the mean free path of electron λ and the reduced electric field E/p. Under the condition of constant temperature, λ is inversely proportional to the number density of gas n, and n depends linearly on air pressure p, so the macroscopic parameter p, which is easy to measure, can be used to represent the microscopic parameter λ, because of $\lambda \propto 1/p$. Hence, pd is proportional to the number of collisions N_c, where d is the distance between the electrodes and E/p is proportional to the energy gained by each electron from every collision. Consequently, the influences of other parameters can be ignored, and as long as pd and E/p are kept the same in different breakdown processes, the number of collisions and the energy gained by each electron from one collision are nearly the same. Then the whole breakdown processes between similar cases are considered to be the same macroscopically, so the premises of the similarity principle in DC-discharges can be written as[10,11]

$$p_1 d_1 = p_2 d_2, \tag{1}$$

$$\frac{E_1(p_1 x_1)}{p_1} = \frac{E_2(p_2 x_2)}{p_2}, \tag{2}$$

Table 1. Relations between parameters of two systems with similar DC discharges.[12,13]

Physical parameters	Similar relations
Number density of particles	$n_1 = n_2/k^2$
Electric field at corresponding position	$E_1(x_1) = E_2(x_2)/k$
Mean free path of particles	$\lambda_1 = k\lambda_2$
Energy gained by each collision	$E_1\lambda_1 = E_2\lambda_2$
Surface charge density of electrodes	$\sigma_1 = \sigma_2/k$
Space charge density	$\rho_1 = \rho_2/k^2$
Current density	$j_1 = j_2/k^2$
Time interval of each process	$dt_1 = kdt_2$

2.2. Premises of similarity principle in microwave breakdown

For the case of microwave breakdown with low pressure, there are two phenomena which are different from those of static discharges. First, the direction of the electric field in microwave band changes so fast that the ions and even the electrons could not reach the cathode within one period, so they just oscillate in the space with the frequency of microwave. Second, the secondary ionization does not play an important role as in the case of static discharge, the breakdown process is determined only by the primary ionization and the loss of electrons caused only by the diffusion to the walls.[7] Hence, the concept of 'electrode' is unimportant in the microwave breakdown, and the actual path traversed by an electron is not determined by the concentration of gas atoms (gas pressure p) nor by the distance between electrodes d, like that in the case of an electron driven by a uni-directional field, but is determined by the microwave frequency f. Thus, as long as f/p and E/p are kept the same, the whole breakdown process is considered to be the same. The relations of the similarity principle in microwave breakdown are[7,8]

$$\frac{f_1}{p_1} = \frac{f_2}{p_2}, \tag{3}$$

$$\frac{E_1(p_1 x_1)}{p_1} = \frac{E_2(p_2 x_2)}{p_2}. \tag{4}$$

In addition, in microwave plasma, there is no need to calculate the surface charge density of an electrode nor current density, which are vital parameters in DC-discharge as shown in Table 1.

3. Modeling

3.1. Breakdown regions and boundary conditions

Figure 1 shows the diagram of the high power microwave (HPM) system for argon breakdown, the microwave with power higher than 1000 W is generated by HPM source, and is transmitted into the breakdown region through a rectangular waveguide. The waterloaded circulator is used to absorb the reflected HPM and guarantee the safety of HPM source.

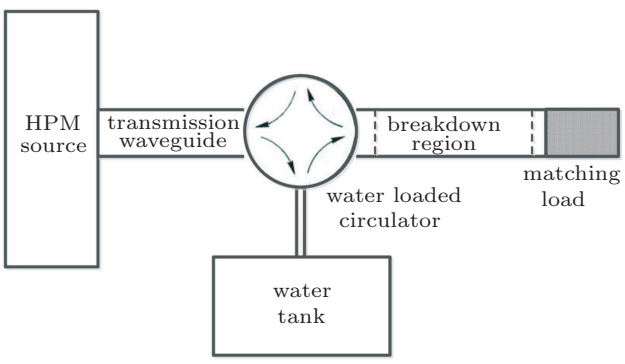


Fig. 1. Diagram of HPM system for argon breakdown.

Figure 2 shows the geometrical structures of the breakdown regions of three similar cases. Here, we refer to the largest one as the prototype case and the smaller two as the scale-down cases, their scale-down factor k values are set to be 2 and 5 respectively. In order to obtain similar breakdowns, f/p and E/p are ensured to be the same. Hence, for the prototype case, $a_1 = 0.25$ m, $b_1 = 0.05$ m, the air pressure $p_1 = 200$ Pa, the power of incident microwave $\text{Power}_1 = 1000$ W, and the frequency of incident microwave $f_1 = 2.45$ GHz. For the scale-down case with $k = 2$, $a_2 = 0.125$ m, $b_2 = 0.025$ m, $p_2 = 400$ Pa, $\text{Power}_2 = 2000$ W, and $f_2 = 4.9$ GHz. For the scale-down case with $k = 5$, $a_3 = 0.5$ m, $b_3 = 0.01$ m, $p_3 = 1000$ Pa, $\text{Power}_3 = 5000$ W, and $f_3 = 12.25$ GHz. Two observation lines l_1 and l_2 are set to be in the regions. For each case, l_1 is set to be on the central axis, l_2 is set to be on the line with one fifth of the distance between two plates of waveguide, which is in close proximity to the lower plate.

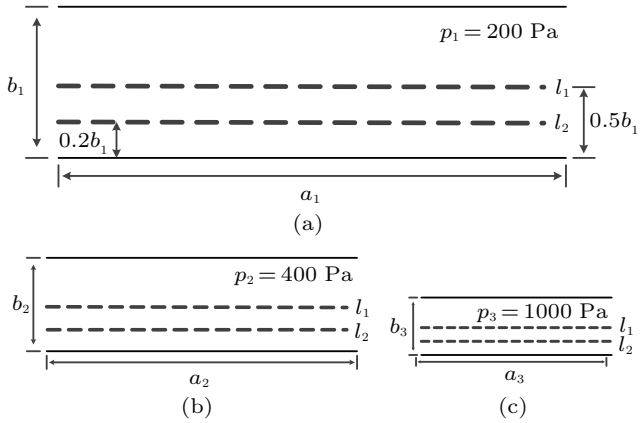


Fig. 2. Schematic diagrams of the similar cases: (a) prototype case, (b) scale-down case ($k = 2$), and (c) scale-down case ($k = 5$).

The computational domain of each case is shown in Fig. 3, where o–a and c–b represent the two plates of the parallel plate waveguide. The fluid equations of microwave plasma are computed in the region of o–a–b–c, and o–c and a–b are set as the waveguide ports for the excitation of incident wave working at TEM mode. Assuming that no reflection occurs on the 'wall' boundary b–c and o–a, which means that for b–c and o–a, zero gradient boundary condition for electrons is used, and the metastable atoms Ar^* and ions Ar^+ are absorbed due to the surface reactions on the wall boundary: $Ar^* \Longrightarrow Ar$ and $Ar^+ \Longrightarrow Ar$. The specific proportionate values for similar cases are shown in Table 2. The gas temperature is set to be 300 K, which approaches the room temperature.

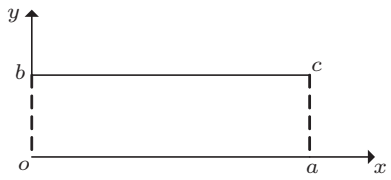


Fig. 3. Computational domain of microwave breakdown.

Table 2. Parameters in similar cases.

Prototype case	Scale-down case ($k = 2$)	Scale-down case ($k = 5$)
$a_1 = 0.25$ m	$a_2 = 0.125$ m	$a_3 = 0.05$ m
$b_1 = 0.05$ m	$b_2 = 0.025$ m	$b_3 = 0.01$ m
$p_1 = 200$ Pa	$p_2 = 400$ Pa	$p_3 = 1000$ Pa
$f_1 = 2.45$ GHz	$f_2 = 4.9$ GHz	$f_3 = 12.25$ GHz
$\text{Power}_1 = 1000$ W	$\text{Power}_2 = 2000$ W	$\text{Power}_3 = 5000$ W

3.2. Fluid model of microwave plasma

The Maxwell equations are[14]

$$\nabla \times E = \frac{\partial B}{\partial t}, \tag{5}$$

$$\frac{\partial D}{\partial t} = \nabla \times H - J. \tag{6}$$

The electron transport equations are[15]

$$\frac{\partial n_e}{\partial t} + \nabla \cdot \Gamma_e = R_e, \tag{7}$$

$$\Gamma_e = n_e(u_e \cdot E) - D_e \cdot \nabla n_e, \tag{8}$$

where n_e is the electron density, R_e is the source of electrons consumed by ionization or recombination, Γ_e is the electron density flux, u_e is the electron mobility, and D_e is the electron diffusion coefficient.

The electron energy transport equations are

$$\frac{\partial n_\varepsilon}{\partial t} + \nabla \cdot \Gamma_\varepsilon + e\Gamma_e \cdot \nabla U = R_\varepsilon, \tag{9}$$

$$\Gamma_\varepsilon = -n_\varepsilon (u_\varepsilon \cdot E) D_\varepsilon \cdot \nabla n_\varepsilon, \tag{10}$$

where n_ε is the electron energy density, R_ε is the source of energy loss caused by the inelastic collision, e is the unit charge, Γ_ε is the electron energy flux, u_ε is the electron energy mobility, and D_ε is the electron energy diffusion coefficient.

The electron source term is given by[16]

$$S_k = \sum_j k_j N_n n_k, \tag{11}$$

where N_n is the number density of target species in the j-th reaction, k_j is the reaction coefficient of the j-th reaction, which can be obtained from the cross sectional data as follows:

$$k_j = \gamma \int_0^\infty \varepsilon \sigma_j(\varepsilon) f(\varepsilon) \mathrm{d}\varepsilon, \tag{12}$$

where $\gamma = \sqrt{2e/m_e}$ is a constant, $\sigma_j(\varepsilon)$ is the cross section of the j-th reaction, and $f(\varepsilon)$ is the electron energy distribution function used in this model.

The electron energy source is given by

$$S_\varepsilon = -q_e \Gamma_e E - \sum_j k_j N_n n_k \Delta\varepsilon_j, \tag{13}$$

where $\Delta\varepsilon_j$ is the energy loss of the j-th reaction, and q_e is the elementary charge.

The equations of heavy particles are given by

$$\rho\frac{\partial w_p}{\partial t}+\nabla\cdot d_p = R_p, \tag{14}$$

$$d_p = \rho w_p v_p, \tag{15}$$

where ρ is the density of gas, p is the heavy particle type, R_p is the production or destruction of particle p in reactions, w_p is the mass fraction of particle p, and d_p is the diffusive mass flux of particle p.

All the reactions calculated by Eqs. (5)–(15) are shown in Table 3. The rates of reactions (1)–(5) in Table 3 can be calculated by the cross section data, and the rate coefficients for reactions (6)–(8) are set to be constant, and their values are 6.4×10^{-10} cm^3·s^{-1}, 2.3×10^{-15} cm^3·s^{-1}, and 1.8×10^{-6} cm^3·s^{-1} respectively. The microwave breakdown model is computed by the finite-element method.

Table 3. Main reactions and particles for argon plasma.[17–22]

No.	Reactions	Description	Δε/eV
1	e+Ar⟹ e+Ar	Elastic collision	
2	e+Ar⟹ e+Ar*	Excitation	11.83
3	e+Ar* ⟹ e+Ar	Superelastic	−11.5
4	e+Ar⟹ 2e+Ar$^+$	One step ionization	15.76
5	e+Ar* ⟹ 2e+Ar$^+$	Step-wise ionization	4.24
6	Ar*+Ar*⟹ e+ Ar+Ar$^+$	Penning ionization	–
7	Ar*+Ar⟹Ar+Ar	Metastable quenching	–
8	Ar* ⟹ $h\nu$+Ar	Radiation	–

4. Results and discussion

The distributions of reduced electric field E/p in similar cases are kept the same by using specific combinations of incident powers and waveguide cross section areas to meet the premise of similarity principle, and their values along the observation line l_1 are shown in Fig. 4. In order to make results more clear, we use px, the product of air pressure p, and position x, as the horizontal ordinate in this figure. From Fig. 4 we can see that the reduced electric fields of the three similar cases are nearly the same in the beginning ($<1\times10^{-10}$ s) and meet the premise of the similarity principle of microwave discharge perfectly. The peak values of E/p in similar cases are 3.13 V·cm^{-1}·Pa^{-1}, 3.11 V·cm^{-1}·Pa^{-1}, and 3.11 V·cm^{-1}·Pa^{-1} respectively. We could obtain that the peak values of electric field are 3.13 V·cm^{-1}·Pa^{-1} at a pressure of 200 Pa for the prototype case, 6.22 V·cm^{-1}·Pa^{-1} at 400 Pa for the scale-down case of $k=2$, and 15.55 V·cm^{-1}·Pa^{-1} at 1000 Pa for the scale-down case of $k=5$. The continued proportion of the three maximum values of electric field is equal to 1:1.99:5. Similarly, we can obtain that at the time of 10^{-6} s, the peak values of electric fields are 3.03 V·cm^{-1}·Pa^{-1} at the pressure of 200 Pa for the prototype case, 4.46 V·cm^{-1}·Pa^{-1} at the pressure of 400 Pa for the scale-down case of $k=2$, and 7.55 V·cm^{-1}·Pa^{-1} at the pressure of 1000 Pa for the scale-down case of $k=5$. The continued proportion of the maximum values of electric field is equal to 1:1.47:2.49. The results show that as time goes on, the breakdown occurs and the deviations begin to show up. At the time of 10^{-2} s, the plasma becomes steady. The peak values of electric field are 0.096 V·cm^{-1}·Pa^{-1} at the pressure of 200 Pa for the prototype case, 0.210 V·cm^{-1}·Pa^{-1} at the pressure of 400 Pa for the scale-down case of $k=2$, and 0.589 V·cm^{-1}·Pa^{-1} at the pressure of 1000 Pa for the scale-down case of $k=5$,

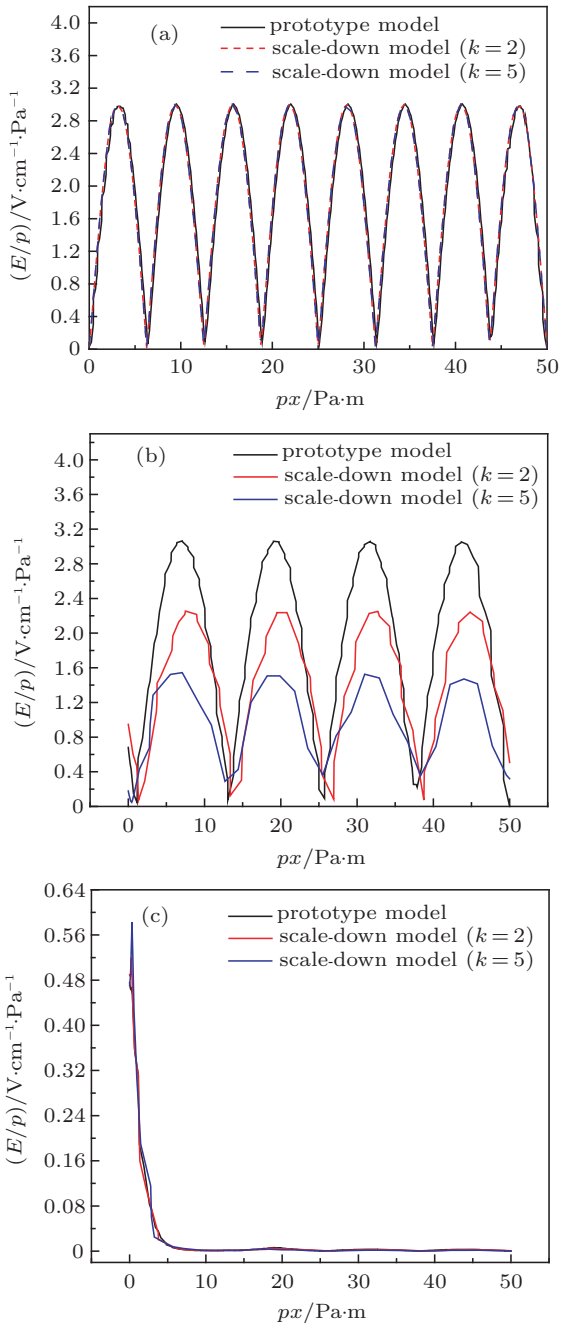


Fig. 4. (color online) Distributions of reduced electrical field along l_1 of three waveguides at different times: (a) 1×10^{-10} s, (b) 1×10^{-6} s, and (c) 1×10^{-2} s.

respectively. The continued proportion of the three maximum values of electric field is equal to 1:2.188:6.13. These proportions of peak values still have a big deviation from the theoretical proportion of 1:2:5, but the reduced electric fields E/p are nearly the same almost everywhere in similar cases at this time as shown in Fig. 4(c).

Figure 5 gives the 2D distributions of electron density in three similar cases. From Figs. 4 and 5, we can see that in the very beginning, free electrons are generated just in the area where the electric field is strong, so the distribution of electrons is similar to that of an electric field. As time goes on, the electron density near the incident terminal keeps growing, and the electric field becomes weaker. This is because when the electron density reaches a certain value, the frequency of electron plasma will be greater than that of incident wave, which prevents the electromagnetic wave from propagating within the plasma.[23,24] The profiles of the 2D distributions of electron density in Fig. 5 are almost the same in three similar cases at any time, which can be a preliminary verification of the similar principle.

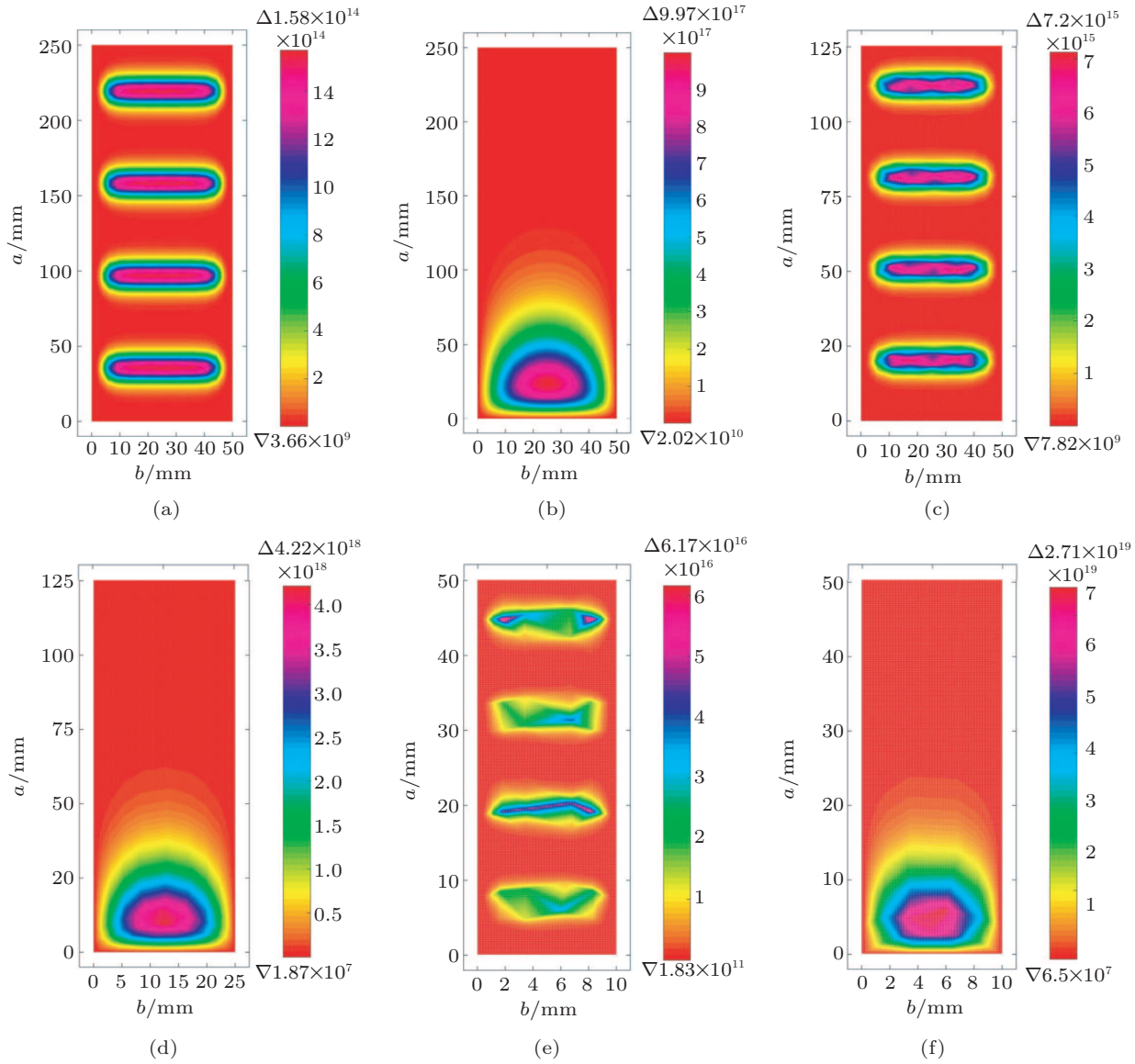


Fig. 5. (color online) Spatial distributions of the electron density in similar cases: (a) $b = 0.05$ m, time = 1×10^{-6} s; (b) $b = 0.05$ m, time = 1×10^{-2} s; (c) $b = 0.025$ m, time = 1×10^{-6} s; (d) $b = 0.025$ m, time = 1×10^{-2} s; (e) $b = 0.01$ m, time = 1×10^{-6} s; and (f) $b = 0.01$ m, time = 1×10^{-2} s.

Comparisons of electron densities along the observation line l_1 at 1×10^{-6} s and 1×10^{-2} s are given in Fig. 6. It can be observed that the discharge regions are quite coincident with the distributions of electrical field shown in Fig. 4. The peak values of electron density are all located near the peaks of electrical field, which means that the excitations and ionizations keep taking place in these regions. According to the relations shown in Table 1, the continued proportion of the values of electric field should be 1:4:25. Taking peak values of electron density along l_1 for example, at 1×10^{-6} s, the electron densities are 1.57×10^{15} m^{-3}, 7.00×10^{15} m^{-3}, and 4.78×10^{16} m^{-3} respectively, the continued proportion of

the peak values of electron density is equal to $1{:}2.11^2{:}5.52^2$. At 1×10^{-2} s, the peak values of electron density are 9.96×10^{17} m^{-3}, 4.21×10^{18} m^{-3}, and 2.66×10^{19} m^{-3} respectively, the continued proportion of the peak values of electron density is equal to $1{:}2.05^2{:}5.17^2$. The ratios of electron density between similar cases satisfy the proportional relations shown in Table 1 very well.

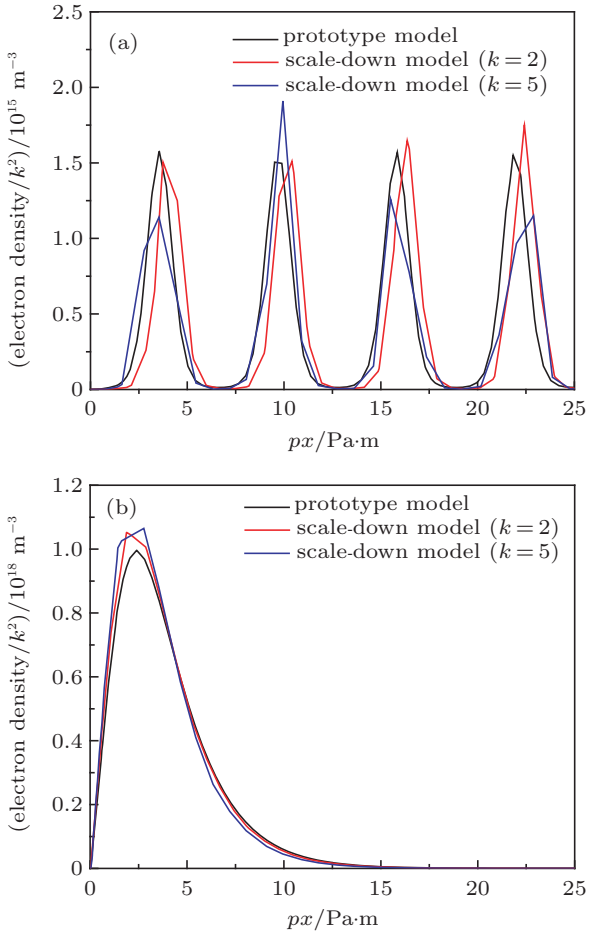


Fig. 6. (color online) Distributions of electron density along observation line1. at (a) 1×10^{-6} s and (b) 1×10^{-2} s.

The electron densities of the three similar cases as a function of time, along the observation lines l_1 and l_2 in the waveguide, are shown in Fig. 7. It is observed that the ratios of electron density to the squared scale-down factor, i.e., n_e/k^2, at the corresponding positions of similar cases for every time moment, are almost the same, which indicates that the ionization processes at every corresponding position of the three cases are similar, and the distribution curves are coincident with each other.

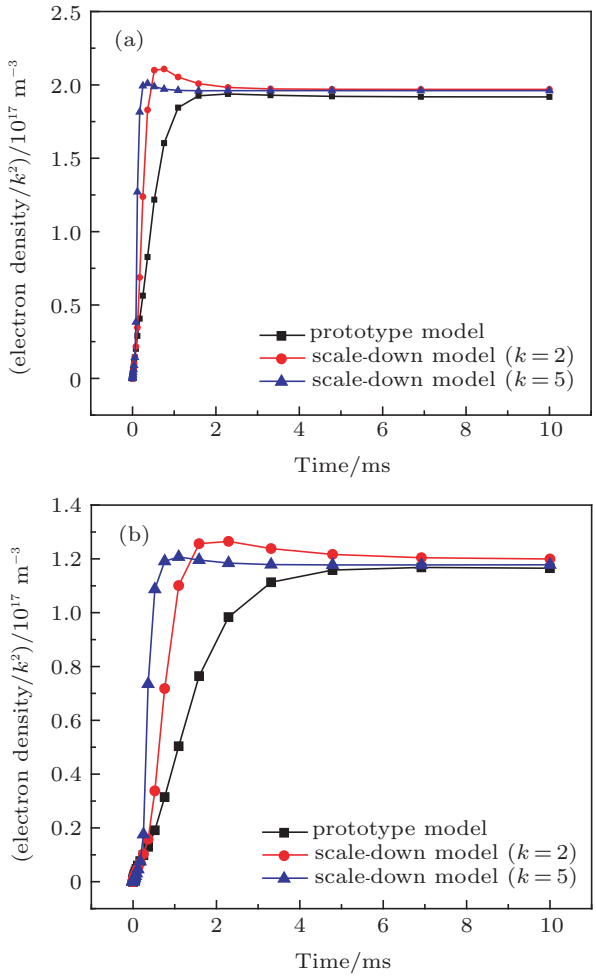


Fig. 7. (color online) Electron densities of similar cases at different times at (a) observation line 1, and (b) observation line 2.

The mean electron density of the whole breakdown region and the ratios of mean electron density to squared scale-down factor of the three similar cases at different times (from 1×10^{-6} s$\sim1\times10^{-2}$ s) are listed in Table 4. The results show that the continued ratio of the similar cases are approximate to $1{:}k_1^2{:}k_2^2$. The maximum deviation is 10% less than the accurate relation of similarity principle, and in most of time period, it is about 5% With the time goes on, the deviation turns smaller.

The mean electron temperatures along the central axis of the three similar cases are shown in Fig. 8. As shown in this figure, the trends of the mean electron temperature in different cases are basically the same at any time, which are consistent with the theoretical relations listed in Table 1.

The electron temperature reaches a peak value of about 5 eV in the prototype case and scale-down case ($k=2$), and

Table 4. Densities of electrons in similar cases and ratios.

Time	Prototype ($k=1$)	Scale-down case ($k=2$)	Scale-down case ($k=5$)	Ratio
1×10^{-6}	4.09×10^{14}	1.51×10^{15}	8.37×10^{15}	$1{:}1.92^2{:}4.52^2$
1×10^{-5}	3.90×10^{15}	1.45×10^{16}	7.37×10^{16}	$1{:}1.93^2{:}4.35^2$
1×10^{-4}	2.89×10^{16}	1.38×10^{17}	5.81×10^{17}	$1{:}1.93^2{:}4.35^2$
1×10^{-3}	1.85×10^{17}	8.21×10^{17}	4.91×10^{18}	$1{:}2.11^2{:}5.15^2$
1×10^{-2}	1.92×10^{17}	7.88×10^{17}	4.90×10^{18}	$1{:}2.02^2{:}5.05^2$

reaches about 5.9 eV in scale-down case ($k = 5$) after the electrons have been accelerated by high power microwave, these accelerated electrons gain enough energy for collisions and reactions listed in Table 3. Then electron temperature decreases because the energy is transferred to other particles rapidly due to frequent inelastic collisions as time goes on. Significant low mean electron temperature at about 0.9 eV is observed in the bulk plasma for all three cases, because the electrons move toward the incident waveguide port as time goes on and reflect most of the incident power. Hence, nearly all the incident energy is blocked in the front part of waveguide. So most of electrons in the remaining part of the waveguide can only gain very limited energy from incident microwave. For the low-pressure microwave breakdown, the generation of the charged particles is mainly determined by the electron ionization, which depends mainly on the electron temperature. Therefore, if the same trend of electron temperature between similar cases is observed, the same energy $E\lambda$ will be obtained and the discharges in similar cases will be comparable to each other. Thus, the similarity principle relation is also valid here in the microwave breakdown at low pressure.

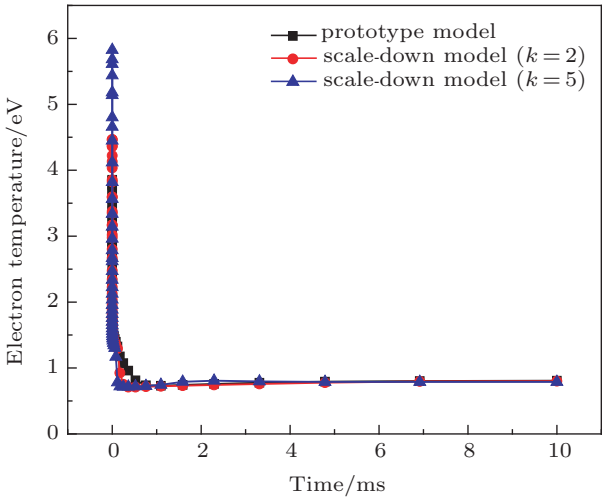


Fig. 8. (color online) Time-dependent mean electron temperatures along the central axis in similar cases.

The similarity principle of the microwave plasma at the steady-state is the focus of this study. The relations of plasma parameters at steady-state among similar cases are checked and confirmed with the similarity theory.

The results discussed above are in good consistence with similarity relations at the steady state of plasma, even though there are clear deviations in transient state. This phenomenon may be caused by the nonlinear processes such as stepwise ionizations in the breakdown process, of which the creation rate of corresponding particles progressively deviates from the prediction of similarity principle, and the deviation turns bigger as the scale-up factor k increases.[25,26] The detailed precondition and application scope of the similarity principle in microwave band will be conducted in in our future work.

5. Conclusions

In this work, the correctness of similarity principle in microwave breakdown is verified, and the premises of similarity principle in microwave breakdown are given. A 2D fluid model of argon plasma is established and three similar cases with a continued proportion of 1:2:5 in size are studied. By comparing the breakdown parameters in these similar cases, the proportional relations in microwave breakdown are found. The electron density distributions and mean electron temperatures of the three cases are approximately the same, the electric field is proportional to the scale-down factor k, and the electron density and ion density are proportional to the squared scale-down factor k^2. The results show that in microwave breakdown, the proportional relations of the similarity principle are similar to those in DC-discharges, but with new premises.

References

[1] Bittencourt J A 1986 *Int. J. Opt.* **28** 881
[2] Townsend J S 1915 *Electricity in Gases* (Oxford: Clarendon Press)
[3] Osmokrovic P 2006 *Plasma Sources Sci. Technol.* **15** 703
[4] Dekić S, Osmokrović P, Vujisić M and Stanković K 2010 *IEEE Trans. Dielectr. Electr. Insul.* **17** 1185
[5] Paschen F 1889 *Ann. Phys.* **273** 69
[6] Holm R 1924 *Phys. Z.* **25** 497
[7] Margenau H 1948 *Phys. Rev.* **73** 326
[8] Jones F L and Morgan G D 1951 *Proc. Phys. Soc., London, Sect. B* **64** 560
[9] Fu Y Y, Luo H Y, Zou X B, Wang X X 2014 *IEEE Trans. Plasma Sci.* **42** 1544
[10] Mezei P, Cserfalvi T, Jánossy M, Szöcs K and Kim H J 1999 *J. Phys. D: Appl. Phys.* **31** 2818
[11] Vitruk P P, Baker H J and Hall D R 1994 *IEEE J. Quantum Electron.* **30** 1623
[12] Mesyats G 2006 *Phys. Usp.* **49** 1045
[13] Mesyats G A 2006 *JEPT Lett.* **83** 19
[14] Zhao P C, Guo L X and Shu P P 2017 *Chin. Phys. B* **26** 029201
[15] Fu Y Y, Yang S, Zou X B, Luo H Y andWang X X 2016 *Phys. Plasmas* **23** 093509
[16] Fu Y Y, Verboncoeur J P, Christlieb A J and Wang X X 2017 *Phys. Plasmas* **24** 83516
[17] Ferreira C M, Alves L L, Pinheiro M and Sá A B 1991 *IEEE Trans. Plasma Sci.* **19** 229
[18] Hyman H A 1979 *Phys. Rev. A* **20** 855
[19] Roberto M, Smith H B and Verboncoeur J P 2003 *IEEE Trans. Plasma Sci.* **31** 1292
[20] Lieberman M A and Lichtenberg A J 2005 *Principles of Plasma Discharges & Materials Processing* (Chichester: John Wiley and Sons) p. 800
[21] Fiala A, Pitchford L C and Boeuf J P 1994 *Phys. Rev. E* **49** 5607
[22] Yamabe C, Buckman S J and Phelps A V 1983 *Phys. Rev. A* **27** 1345
[23] Liu S B, Mo J J and Yuan N C 2002 *Int. J. Infrared Millimeter Waves* **23** 1803
[24] Kim H C and Verboncoeur J P 2007 *Comput. Phys. Commun.* **177** 118
[25] Fu Y Y, Parsey G M, Verboncoeur J P and Christlieb A J 2017 *Phys. Plasmas* **24** 113518
[26] Fu Y Y, Luo H Y, Zou X B and Wang X X 2014 *Plasma Sources Sci. Technol.* **23** 065035